A STUDY OF THE PHOTOCHROMIC AND

PHOTOREFRACTIVE EFFECTS IN

BORON-DOPED BISMUTH

SILICON OXIDE

By

ANNE MARIE GEORGALAS
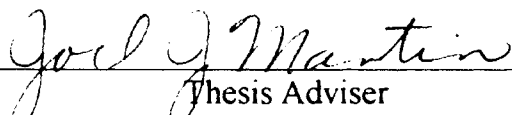
Bachelor of Science

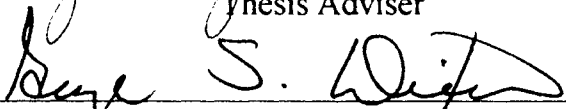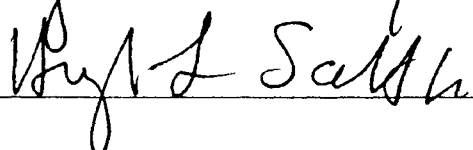Cleveland State University

Cleveland, Ohio

1992

Submitted to the Faculty of the
Graduate College of the
Oklahoma State University
in partial fulfillment of
the requirements for
the Degree of
MASTER OF SCIENCE
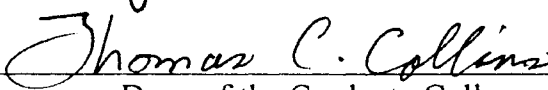December, 1994

A STUDY OF THE PHOTOCHROMIC AND

PHOTOREFRACTIVE EFFECTS IN

BORON-DOPED BISMUTH

SILICON OXIDE

Thesis Approved:

Joel J Martin
Thesis Adviser

Bruce S. White

Wright L Smith

Thomas C. Collins
Dean of the Graduate College

ACKNOWLEDGMENTS

This past year, I have had the pleasure of working with my adviser and committee chairman, Dr. Joel J. Martin. He is an incredible teacher with an extraordinary amount of insight and patience. I wish to thank him for his guidance and encouragement throughout my studies.

I would also like to express my appreciation to Dr. George Dixon and Dr. Larry Scott for serving on my committee. Thanks also to Mr. Charles A. Hunt for his patience and technical proficiency and to Mr. Mike Hamilton for his incredible programming skills. And a special thanks to Dr. David W. Hart, who was never too busy to fix any disaster--no matter how small--or answer any question--no matter how dumb.

My sincere thanks goes to Dr. Jearl D. Walker for his constant optimism and for first showing me how fascinating physics can be. For a never-ending amount of support at all hours of day and night, I want to thank Michael Furlough, John Snodgrass, Jeff McCullough, Cindy Porter, Sheena Jacob, Steve Willoughby, Rob Wolf, Susan Hoefler, Roger Vogel, Carolyn Thompson, and Imtiaz Shaikh.

This whole project would have been impossible without the love and support of my family and especially my brother, Louis, for everything ranging from computer advice to long phone calls to regular visits.

iii

TABLE OF CONTENTS

LIST OF TABLES

LIST OF FIGURES

CHAPTER I

INTRODUCTION

Bismuth silicon oxide, $Bi_{12}SiO_{20}$, BSO, is a photorefractive material of current interest for optical signal processing applications. Other studies have shown that BSO exhibits photoconductivity [1], photoluminescence [2], thermally stimulated currents and luminescence [3], optical activity, and Faraday rotation [4]. Its properties are similar to those of the related compound bismuth germanium oxide, $Bi_{12}GeO_{20}$., BGO, although BSO has a higher resistivity and better electro-optic properties [5].

BSO has a body-centered cubic structure known as sillenite, named for Sillen who first studied the material [5]. The structure corresponds to space group 23, meaning the crystal exhibits two-fold symmetry along one axis and three-fold symmetry along another. The unit cell consists of two full chemical formula. The corners and center of the body-centered frame contain silicon atoms. Each silicon atom is surrounded by four oxygen atoms lying along the cube diagonals. This forms a perfect tetrahedra. Each bismuth atom is surrounded by seven oxygen atoms, forming a distorted octahedra. BSO lacks inversion symmetry and so it is piezoelectric and electro-optic [5].

Recently, studies have been conducted to identify the photochromic bands in BSO doped with various substances, including the Group IIIA elements aluminum and gallium. The photorefractive effect is also being studied using these dopants.

Defects

BSO, BGO, and other insulating materials adhere to the following model. A pure electrical insulator has a completely full valence band and a completely empty conduction band separated by an energy gap, E_g. However, insulators can contain certain impurities or defects which can contribute electrons to the conduction band or holes to the valence band. A donor impurity has an extra electron in a level within the energy gap. When the crystal is exposed to optical or thermal energy with a donor energy, E_d, these electrons are excited into the conduction band. They migrate in this band until they recombine at an empty shallower trap. Similarly, impurity sites called acceptors trap electrons from the valence band and leave holes behind to migrate through the valence band.

Czochralski-grown undoped BSO is yellow in color due to an absorption shoulder that extends from approximately 2.5 eV to 3.4 eV. This absorption shoulder is caused by a deep donor. This donor is thought to sit about 2.8-2.9 eV below the conduction band. The separation of the conduction and the valence band is about 3.4 eV.

Hydrothermally-grown undoped BSO is colorless, though, because the deep donor absorption shoulder is missing according to a recent study by Harris, Larkin, and Martin [6]. Additionally, band gap or ionizing radiation does not produce more absorption bands. Their study concludes that the density of traps responsible for photochromic absorption in Czochralski-grown materials is much less in hydrothermally-grown. However, when a crystal was pulled from a melt of hydrothermal material the yellow

coloration returned and its low temperature photochromic response was similar to the Czochralski-grown crystals.

The nature of the donor is not understood. Hou, Lauer, and Aldrich [7] attributed the shoulder to a vacancy complex, V_{Si} -V_O, which was considered to be the donor center. When a 5% aluminum BSO crystal was grown, the authors found that the shoulder had disappeared. This bleaching was attributed to a charge compensation produced by the aluminum ions sitting at the vacancy complex . Grabmaier and Oberschmid [8] and Rehwald, *et al.* [9] confirmed these results for aluminum-doped BSO and found similar results for gallium-doping .

Oberschmid had a different explanation of the deep electron donor. Oberschmid [10] proposed that this deep donor is a bismuth atom on a silicon site, Bi_{Si} . This suggestion is reasonable because a crystal of undoped BSO contains 12 times as much bismuth as silicon according to stoichiometry. This explanation is also based on X-ray studies which indicate that only 87% of the silicon sites in undoped BSO are actually occupied by silicon [11]. A recent paper by Reyher, Hellwig, and Thiemann also concludes that the deep donor is a bismuth sitting at a silicon site [12]. A similar situation occurs in BGO with the deep donor being a bismuth atom on a germanium site, Bi_{Ge}.

In terms of Oberschmid's model, doping with 1-5% gallium or aluminum causes the gallium or aluminum to fill an empty silicon site and act as an acceptor. This electronically compensates the deep donor and removes the absorption shoulder and with it the yellow coloration. If the doping concentration is too low, however, not all the

donors are compensated by acceptors and the absorption shoulder remains. Doping with gallium or aluminum also removes the yellow coloration in BGO.

Defects and Photochromic Bands

The absorption shoulder extends from about 2.5 eV to the band edge at 3.4 eV. When a sample of undoped BSO is illuminated with light between these energies at 80 K, a broad absorption band is induced across the visible spectrum. This band has a peak at 2.6 eV and is associated with one of the traps. The samples appear black due to this photoinduced absorption [13].

The same experiment was performed on undoped BSO at a temperature of 10 K by Hart, *et al*. The spectrum appears to consist of several absorption bands: one in the infrared range at 1.5 eV caused by shallow traps and a much stronger broad one in the visible range near 2.6-2.7 eV caused by the deeper traps. These broad bands are likely made up of several overlapping bands. Individual Gaussian bands were calculated at 1.53, 1.9, 2.2, 2.6, and 3.0 eV but it is more probable that the spectrum consists of a larger number of closely-spaced levels. There are two major anneal stages. The bands at 1.5 eV have a major decay between 110 and 150 K. As these traps decay, some of the electrons are retrapped in the deeper traps so that the band in the visible region is enhanced. The second anneal stage occurs between 220 and 250 K when the visible band decays along with the small remaining infrared band. These results are nearly identical to those found for undoped BGO [14].

Doping BSO with aluminum and gallium has been extensively studied because they compensate the deep donor in undoped material. Martin, Foldvari, and Hunt observed photo-induced absorption bands at 1, 1.38, and 2.45 eV for aluminum-doped BGO. The two infrared bands decay between 80 and 100 K. A major portion of the visible range band decays in this temperature range too. The remainder of the visible band decays between 175 and 240 K [15]. Hart, *et. al.* obtained very similar results for aluminum-doped BSO. They found the same Gaussian bands at 1.0, 1.38, and 2.45 eV that annealed in the same temperature regions as for the aluminum-doped BGO [14].

Hart, Hunt, and Martin then performed the same type of experiments on gallium-doped BGO. They found that BGO doped with less than 4% gallium behaves like undoped BGO. Once BGO was doped with 4% gallium they found an absorption band further into the infrared near 1.1 eV. This is similar to the one found in aluminum-doped BGO. In addition, the same broad band found in aluminum-doped BGO is present in gallium-doped BGO. Gaussian band contributions were calculated at 1.1, 1.55, and 2.45 eV. As with aluminum-doped BGO, the two infrared bands and a major part of the visible band decay together. In gallium-doped BGO, however, this first anneal stage occurs between 100 and 120 K. The remaining portion of the visible band anneals just below 230 K [16].

Martin, *et. al.* [15] suggest that the infrared bands found in aluminum-doped BGO are due to the same type of hole center found in quartz. Band-gap light would excite the electron into the conduction band where it would drift until trapped and leave behind a hole trapped at the aluminum. This hole center is designated $[AlO_4]^0$, using Weil's notation [17]. In analogy with the $[AlO_4]^0$ center in aluminum, Hart, Hunt, and Martin

[16] proposed a similar center for gallium-doped BGO, $[GaO_4]^0$. The 1.38 eV band in aluminum-doped BGO and the 1.55 eV band in gallium-doped BGO are likely not associated with these hole centers. The 2.45 eV absorption band in both aluminum- and gallium-doped BGO and BSO is probably the same absorption band as that found at 2.6 eV in undoped BGO and BSO. But the 1.0 eV and 1.1 eV bands in aluminum- and gallium-doped, respectively, are associated with these hole centers [18]. Hart, *et. al.* [16] believe that gallium-doped BSO behaves nearly identically due to the same gallium hole center.

Defects and the Photorefractive Effect

The photorefractive response in sillenites was first reported by Huignard and Micheron in 1976 [19]. The photorefractive effect is a reversible nonlinear process consisting of a light-induced change in the index of refraction, created by a combination of the electro-optic properties and inherent or introduced defects. The effect has been observed in many electro-optic materials, including BSO and BGO, and is now considered a general property of them. These index changes may be induced by visible light as well as by ultraviolet or infrared radiation, depending on the impurity content [20].

The photorefractive effect is directly related to the defect physics of the material. Early models of the photorefractive effect in sillenites proposed that only one type of charge carrier and one type of trap was participating in the redistribution of charge. But recently investigators have shown that both electrons and holes and shallow and deep

traps participate in the photorefractive effect. When light illuminates the sample, charges are released from impurity ions. Electrons migrate to the dark regions where they are retrapped. The holes also migrate but at a slower rate due to their lower mobility. This separation of charge gives rise to an electrostatic field, creating an added component to the crystal's internal electric field and resulting in the creation of a diffraction grating. This electrostatic field eventually prevents further charge separation. The index of refraction of the material consequently changes because of the linear electro-optic (Pockels') effect, causing a different index of refraction for the bright and dark regions of the created grating. The process known as dark decay occurs after the light is removed. The holes continue their migration in the electrostatic field of the electron grating until they perfectly compensate the electrons and the grating disappears [21], [22].

Both electrons and holes contribute to the photorefractive effect in BSO, although the number of electrons in undoped BSO is approximately an order of magnitude greater than the number of holes [1]. Consequently, undoped BSO is considered to demonstrate n-type photo-conductivity [22]. Doping BSO with enough aluminum or gallium, however, contributes holes that fully compensate the absorption shoulder. All these excess holes cause the doped compound to exhibit p-type photo-conductivity and, therefore, there should be no photorefractive response in compounds where the absorption shoulder is completely compensated [8]. This implies that BSO that has been heavily-doped with aluminum or gallium so that the absorption shoulder is removed should not exhibit a photorefractive response when blue or green light is used for excitation. Experimental results agree with this expectation. No photorefractive signal

could be found when an Argon-ion laser was used to write a grating to BSO heavily-doped with aluminum [22].

Purpose of Investigation

Boron is the lightest of the Group IIIA elements with aluminum and gallium following it in the periodic chart. The purpose of this study was to dope bismuth silicon oxide with two different concentrations of boron to study the production of the photochromic bands using near-band-edge light and the temperatures at which they anneal using optical absorption techniques. This study also examined the photorefractive effects by inducing a diffraction grating using a four-wave mixing experiment. The results of these experiments were used to try to determine the defect structure of boron-doped bismuth silicon oxide.

CHAPTER II

EXPERIMENTAL PROCEDURE

Sample Preparation

For this study, two different concentrations of boron-doped BSO crystals were

grown in air using the Czochralski method. The starting host materials were Johnson-

Mathey Grade-1 Bi_2O_3 , bismuth oxide, and SiO_2, silicon oxide. Boron doping was

carried out by adding boron trioxide, B_2O_3, to the melt according to the formula

$$6Bi_2O_3 + (1-x) SiO_2 + (x/2)B_2O_3.$$
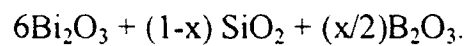
where x is the doping concentration of boron, 0.05 for 5% boron and 0.08 for 8% boron.

Each crystal was to weigh 120 grams. Using the above equation and the molecular

weights of the three compounds, mixtures containing 5% and 8% boron were prepared.

The powders were thoroughly mixed by tumbling them in a motor-driven glass jar for

forty-eight hours and then they were placed in a platinum crucible in an oxygen

atmosphere at 800° C and treated for an additional forty-eight hours.

A seed of undoped BSO with a [100] surface was attached to the pull rod of the

growth chamber. The melt was heated by a radiofrequency induction furnace and the

temperature controlled by an Accufiber model 10 controller using a sapphire sensor in

contact with the bottom of the platinum crucible. The set points for the warm-up ramp,

temperature-time profile during growth, and cool-down ramp were controlled by a Hewlett Packard model 86 microcomputer, programmed in HP-BASIC.

The melt in the platinum crucible was raised to its melting point until it was totally molten: 905° C for the 5% crystal and 888° C for the 8% crystal. The rotating seed was dipped into the melt and slowly lifted from it at a constant rate of 1 mm per hour so that a crystal would form. A rotation rate of 30 to 86 rpm was used. During the initial growth period of several hours, the temperature was lowered at a rate of about 0.0333 degrees per minute. After the first 6 hours, the temperature was decreased at a slower rate--0.0017° C for the 5% crystal and 0.0120° C for the 8% crystal--for an additional day. The lift rate was maintained at 1 mm per hour throughout the growth process. These conditions produce crystals with a prismatic shape: thinner at the top when the temperature decreased faster and then gradually filling out to a wide round base as the temperature decreased slower. When the crystal was completely pulled from the melt, the growth chamber was allowed to slowly cool for 48 hours so the crystal would not crack due to an abrupt temperature change.

The 5% crystal emerged perfectly from the melt and a sample of about 1.5 mm was cut from it at 45° (corresponding to a [110] surface) using a diamond saw. It was optically polished to a thickness of 1.13 mm. Serious problems developed during the growth of the 8% sample. About eight hours into the growth period a water pipe inside the RF induction furnace burst, halting the growth process and rendering the furnace inoperable for several months. Fortunately, the crystal had been pulled about 8 mm from the melt and several usable samples were recovered. The 8% sample used to study the photochromic bands was cut at 45° and polished to a thickness of 0.41 mm. However,

no photorefractive signal could be measured using this sample so a separate sample from the same 8% crystal was cut at 45° and polished to a thickness of 1.03 mm. The 5% and both the 8% samples exhibit the yellow coloration of undoped BSO and are of good optical quality.

Optical Absorption Technique

Optical absorption was carried out using the Cary 5 spectrophotometer with Cary05 software. Two light beams are measured by the spectrophotometer. One beam is a reference beam that is unaffected by the sample. The initial and final intensity are the same: I_o. The other beam is the sample beam which shines through the sample. The initial intensity is I_o and the final is I. The Cary 5 spectrophotometer records the wavelength and the transmission of the light. The transmission relates these intensities by

$$\text{transmission} = I/I_o$$

The operator then converts the files into ASCII for use with other computer languages. In addition, a Hi-Tech BASIC program was written to convert the transmission data into absorbance data using the formula

$$A = \text{absorbance} = -\log(\text{transmission}).$$

The absorbance is also known as the optical density of the sample. Finally, plotting programs also written in Hi-Tech BASIC use this data to find the absorption coefficient, α, using the equation

$$\alpha = (2.303)A/t,$$

where 2.303 is ln 10, a conversion between the two different logarithms and t is the thickness of the sample.

The experimental setup is shown in Fig. 1. Individual samples were mounted on the cold finger of a CTI closed-cycle cryogenic refrigerator so that they were at a 45° angle to the sample beam of the Cary 5 spectrophotometer used for the absorption measurements. This choice of mounting angle allowed the sample to be exposed to the excitation light beam without removing the cold head from the spectrophotometer.

The monochromatic light source for the excitation of the photochromic bands consisted of an Oriel 220 Watt Xenon lamp and a Spex Minimate monochrometer with 2.5 mm slits. A lens was added to the monochrometer to better focus the beam. All optical absorption scans were performed with the sample held at 14-17 K.

The described set-up was used to perform low-temperature absorption measurements first in the as-grown condition and then after exposing each sample to near-band-edge light while the temperature was at 14-17 K, thereby "writing" photochromic bands to the samples. Absorption scans were taken after 5, 15, 30 and 60 minute exposure periods. Plots of absorption coefficient versus energy and difference in absorption coefficient versus energy were made to determine the energy at which the greatest excitation occurred.

The thermal stability of the photochromic bands was also measured with this set-up by carrying out anneals while holding the excitation energy constant at the energy of greatest excitation. Each sample was exposed to near-band-edge light at the previously determined energy of greatest excitation at low temperature for an hour. An absorption spectrum was taken and then the temperature of the cold finger was raised to a desired

value and then returned to 14 K for the next absorption scan. This was performed in 20-30 K intervals until room temperature was reached. The temperature was controlled by a Lakeshore Model 330 Temperature Controller and the CTI closed cycle cryogenic refrigerator was run by a Hi-Tech BASIC program.

Photorefractive Technique

Photorefractive effects were measured using the setup in Fig. 2. This setup is referred to both as four-wave mixing and as laser-induced holographic gratings. The samples were mounted on the cold finger of a CTI Cryogenic refrigerator so that they were oriented perpendicular to the incoming laser beams.

The geometry of the setup was determined using a Hi-Tech BASIC program. A 442 nm Helium Cadmium laser was first sent through a shutter. A grating spacing of 2 microns was chosen and the "write" angle or the angle of the Helium Cadmium laser was determined. This beam was then sent to a beam splitter. Mirrors were used to align these two "write" beams so that they crossed on the sample to form a grating. A 632.8 nm Helium Neon laser was used to "read" the grating. The "read" angle, measured from one of the "write" beams, was determined using Bragg's Law:

$$2D\sin \theta = \lambda,$$

where D is the grating spacing, θ is the "read" angle, and λ is the wavelength of the Helium Neon laser. The Bragg angle is approximately 9°. A neutral density filter was used to reduce the intensity of the "read" beam. The resulting refracted beam was sent to a photomultiplier tube connected to a Hewlett Packard Oscilloscope and a Keithley

Digital Multimeter. The resulting data was analyzed by a Hi-Tech BASIC program. This setup allowed several parameters to be varied throughout the experiment. Sending the "write" beam through a shutter allowed the time the beam was exposed to the sample to be controlled. The intensity of the "write" beam was determined by placing an attenuator between the beam and the shutter. The temperature of the sample was also controlled using the refrigerator.
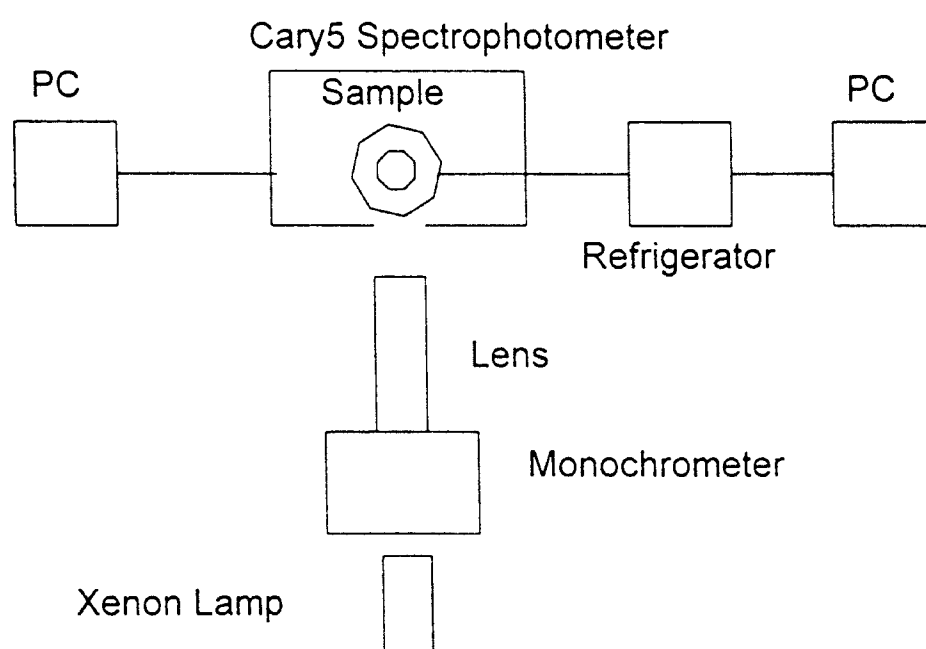
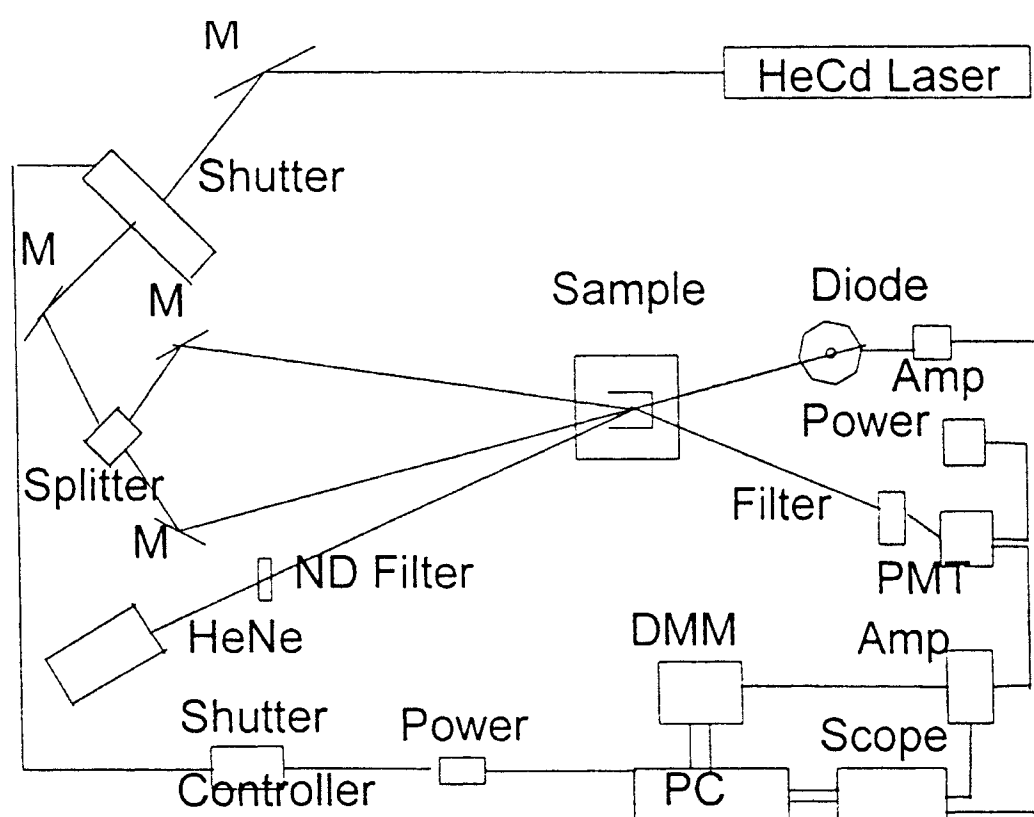Figure 1. Experimental setup for optical absorption measurements.

M

HeCd Laser

Shutter

M

M

Sample   Diode

Amp
Power

Splitter

Filter

M

PMT

ND Filter

HeNe

DMM   Amp

Shutter   Power

Scope

Controller   PC

Figure 2. Experimental setup for photorefractive measurements.

CHAPTER III

RESULTS AND DISCUSSION

Photochromic Bands

Absorption spectra were taken at approximately 14 K on both the 5% and 8% boron samples using the described setup for the Cary 5 spectrophotometer. An absorption scan was first taken on the samples in the as-grown condition. Fig. 3 is a comparison of the curves for undoped BSO, aluminum-doped BSO, and the 8% boron-doped sample. The curve for the aluminum-doped sample shows that the deep donor is fully compensated. It was expected that the 8% boron sample at least would also compensate the deep donor. However, the as-grown curve for the boron-doped sample most closely resembles the curve for undoped BSO and the shoulder on the absorption edge which causes the yellow coloration is definitely present in the boron-doped sample. However, the absorption shoulder is lower in the boron-doped sample. Rehwald, *et. al.* [9] also found a weak compensation of the absorption shoulder for their boron crystal when they performed optical absorption measurements at liquid nitrogen temperatures.

Each sample was then exposed to near-band-edge light for 5, 15, 30, and 60 minutes. Absorption scans were taken after each time interval. Light of 2.8 eV was used for the 5% boron sample while 3.2 eV light was used for the 8% boron sample. Figs. 4 and 5 show the low-temperature absorption spectra taken on 5% and 8% boron, ranging

from the as-grown background curve to the curve taken after 60 minutes exposure to

near-band-edge light. Both curves' responses are nearly the same as that reported for

undoped BSO [14]. Gallium- and aluminum-doped BSO are both known to glow when

they are illuminated with near-band-edge light but no glow was ever observed with either

of the two boron samples.

Figs. 6 and 7 show the spectra of the photochromic absorption bands obtained by

taking the difference between each curve exposed to the light and the background curve.

The maximum photochromic absorption for both samples occurs in the 2.6-2.7 eV range.

Separate difference spectra for the 5% and 8% boron samples are shown in Figs. 8 and 9.

These are obtained by subtracting the background curve from just the 60-minute

exposure curve. The spectra appear to be made up of several overlapping absorption

bands ranging from 1.11 eV to 3.10 eV. This possibility is illustrated by the dashed

curves which show the individually calculated Gaussian bands and their resulting

composite. All but one of the same band positions and half-widths that Hart, *et al.* [14]

used for undoped BSO were used for the two boron samples. In addition, the 2.45 eV

band from BSO doped with 10% aluminum that Hart, *et al.* [14] used was also

incorporated into the Gaussian composite. The strengths of the bands were slightly

adjusted to better match the experimental curves. These parameters are given in Tables I

and II.

TABLE I

GAUSSIAN BAND PARAMETERS FOR 5% BORON

Band (eV)	Half-width (eV)	Strength (cm^{-1})
1.11	0.46	0.50
1.45	0.35	0.70
1.78	0.60	0.60
2.15	0.50	1.80
2.45	1.75	0.50
2.65	0.60	3.40
3.10	0.25	0.15

TABLE II

GAUSSIAN BAND PARAMETERS FOR 8% BORON

Band (eV)	Half-width (eV)	Strength (cm^{-1})
1.11	0.46	0.15
1.45	0.35	0.70
1.78	0.60	0.70
2.15	0.50	2.05
2.45	1.75	0.90
2.65	0.60	3.60
3.10	0.25	1.10

Isochronal anneal studies were performed to investigate the thermal stability of the traps that cause the absorption bands. Anneals were performed by first illuminating the sample at 14 K and measuring the absorption coefficient. The temperature of the sample was raised in 20-30 K steps and then lowered to 14 K again. Scans were taken after returning to 14 K each time. The contour plots in Figs. 10 and 11 show the photochromic absorption bands after subtracting the background curve as a function of anneal temperature for 5% and 8% boron, respectively. For the 5% boron sample, photochromic absorption bands were "written" to the sample by exposing it to 2.8 eV light for one hour. As can be seen from Fig. 10, the infrared bands decay totally in the 120-150 K range. This is accompanied by an enhancement of the bands in the 2-3 eV range. These visible bands begin to decay in the 200-235 K range and finish decaying by about 250 K. The anneal plot for the 8% boron sample is shown in Fig. 11. The photochromic bands were "written" to the sample by exposing it to 3.2 eV light for one hour. The infrared bands decay totally in the 130-175 K range. This decay is accompanied by the same enhancement of the visible range bands that was observed in the 5% boron sample. As with the 5% boron sample, these visible bands decay in the 200-235 K temperature range and finish decaying by 250 K. These results for both boron samples agree very well with the anneal data that Hart, *et al.* [14] obtained for undoped BSO.

The above results for the photochromic bands suggest a picture of the energy levels in boron-doped BSO. Fig. 12 shows an energy level diagram for BSO illuminated with near-band-edge light. The energy level of the donor is shown at about 3.0 eV. The proposed energy level for the acceptor state created by doping BSO with boron is also

shown but is simply labeled as "E". The exact level was not determined since the response of boron-doped BSO was so similar to that for undoped BSO. However, the results do show that there is a partial compensation of the donor and so the acceptor state created by doping with boron must sit below the donor level. It is possible that the acceptor level is only slightly below the donor level but there is no way to tell from the results.

Previous experiments have shown that doping the melt with 3-5% aluminum or gallium is enough to fully compensate the deep donor [14], [16]. It was expected that the same would occur for doping with boron. One possible reason that only a partial compensation of the absorption shoulder occurs even when doping with 8% boron is that the covalent tetrahedral bond radius of boron is significantly shorter than for aluminum or gallium and it is not possible to incorporate sufficient boron to fully compensate the donor. Table III is a comparison of the bond radii for silicon and several Group IIIA elements [23].

TABLE III

COVALENT TETRAHEDRAL BOND RADII

ELEMENT	RADII (10^{-10} m)
SILICON	1.17
BORON	0.88
ALUMINUM	1.26
GALLIUM	1.26
INDIUM	1.44

The silicon-oxygen bond in BSO has a length of 1.65 angstroms. Replacing the silicon with either a gallium or an aluminum increases the bond length by only about 0.09 angstroms. But replacing the silicon with a boron decreases the bond length by about 0.3 angstroms, which is a 20% decrease. This may reduce the solubility of boron in the BSO or it may "drag" along a bismuth into the next silicon site. This is similar to what occurs for the compound $Bi_{25}FeO_{40}$ One study found that this compound has the same structure as BSO with Fe on one silicon site and Bi on the other in the cubic unit cell and so is more clearly written $Bi_{24}(BiFe)O_{40}$ [24]. The antisite bismuth acts as a donor while the antisite iron acts as an acceptor. This excess bismuth that the boron causes to shift makes it impossible to achieve full compensation. For these reasons, boron does not go into BSO very well and it may be impossible to fully compensate the deep donor. Further experiments with greater concentrations of boron in the melt should be attempted to test this hypothesis. Doping BSO with indium should also be carried out to see if a 0.2 angstrom increase in the bond length would allow for full compensation of the deep donor or if this increase also distorts the bonds too much.
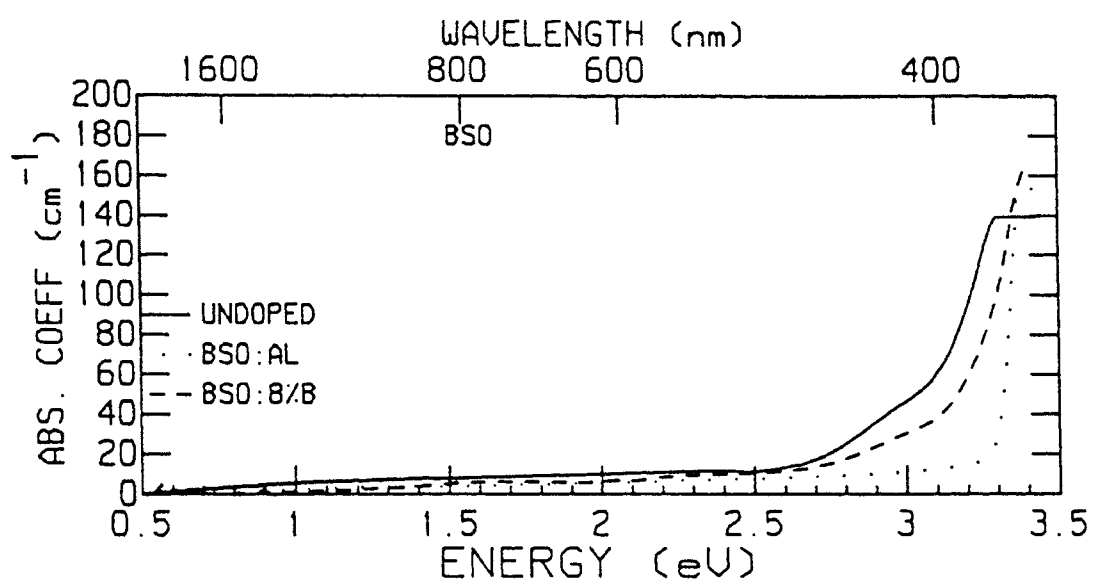
Figure 3. Comparison of the baseline curves for undoped and doped BSO.
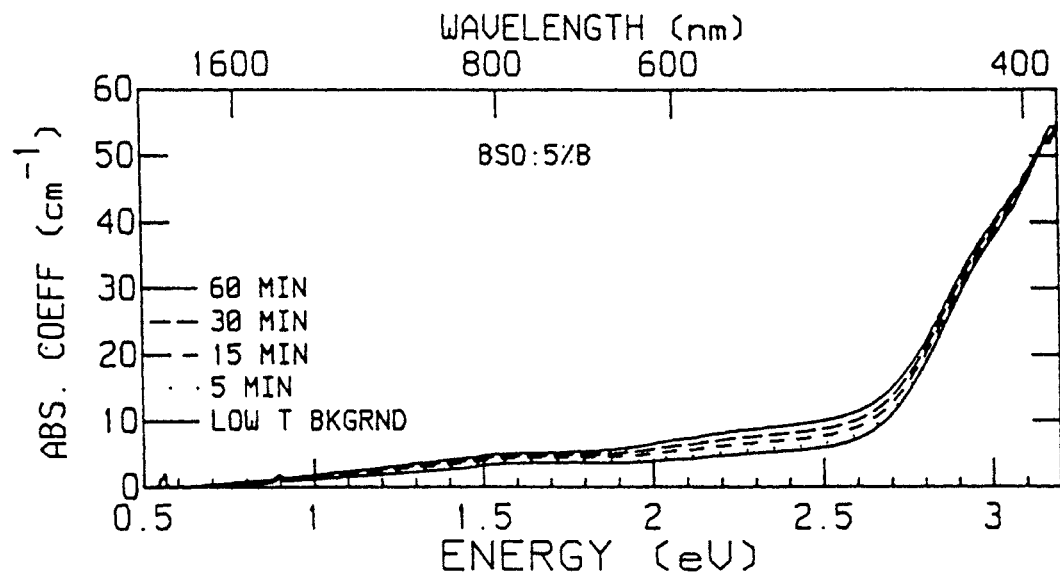
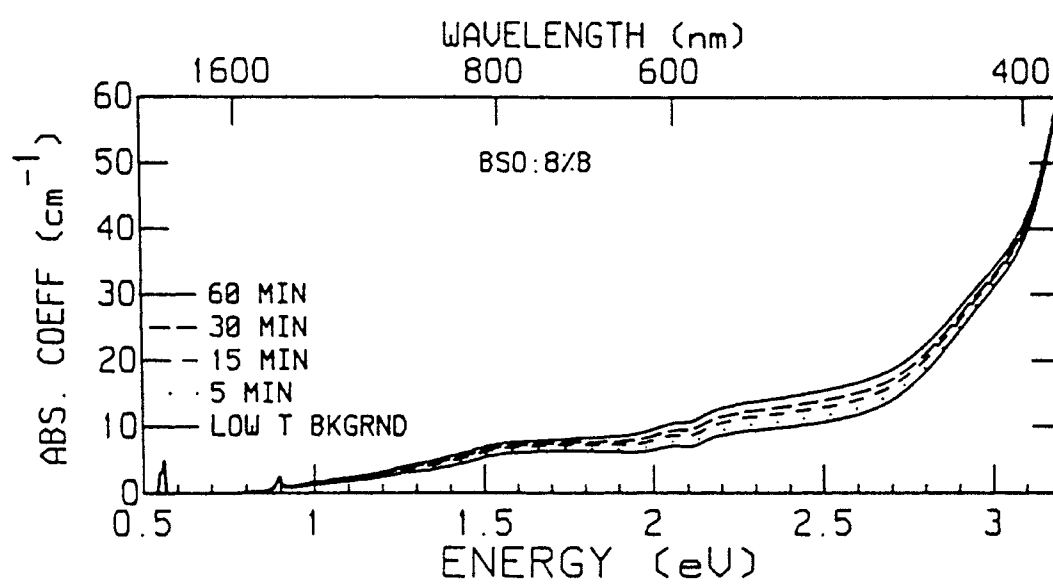Figure 4. Absorption spectra for BSO:5% Boron.
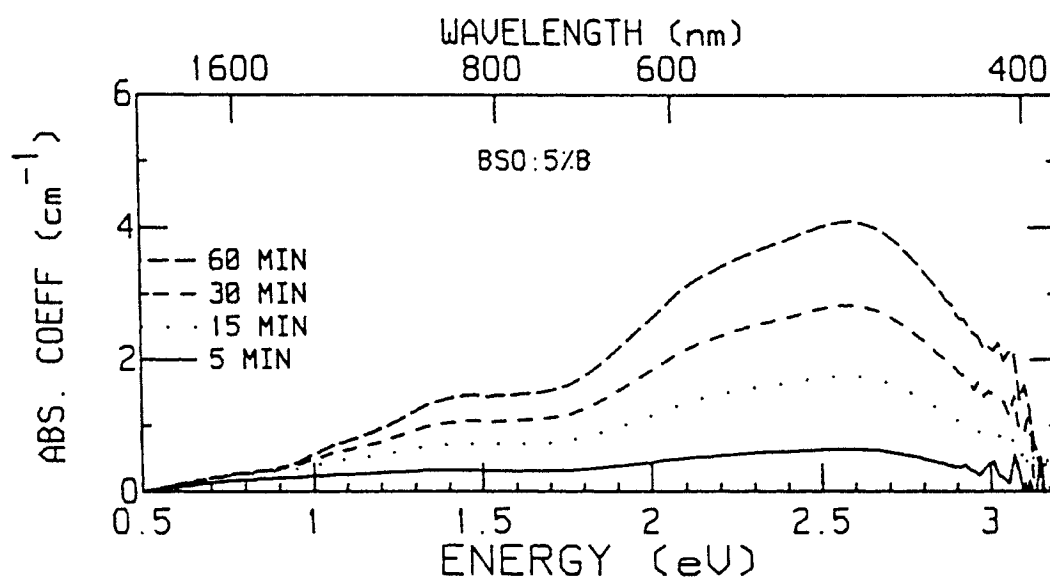
Figure 5. Absorption spectra for BSO:8% Boron.

Figure 6. The change in the absorption spectra for BSO:5% Boron.
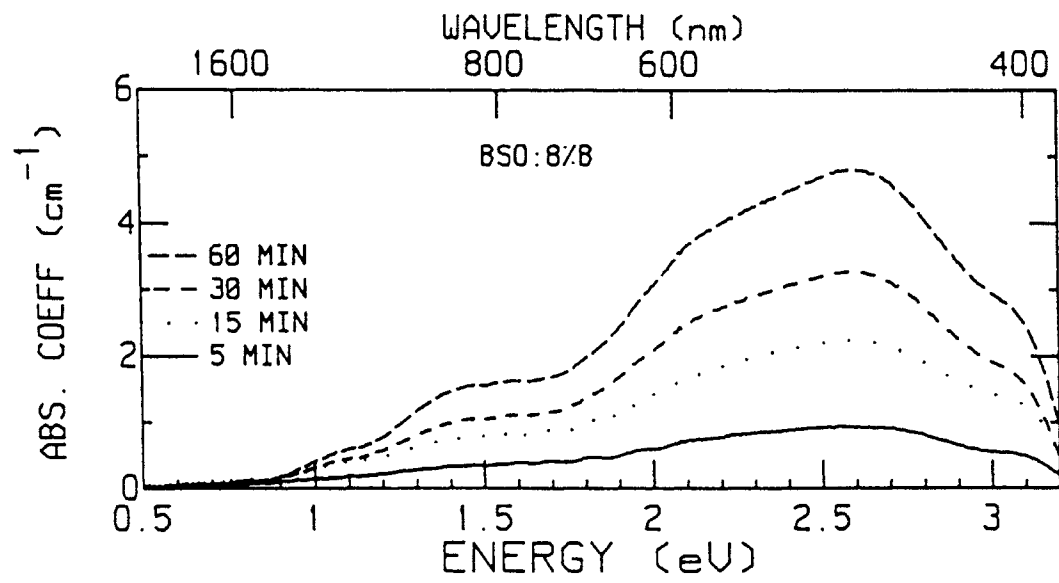
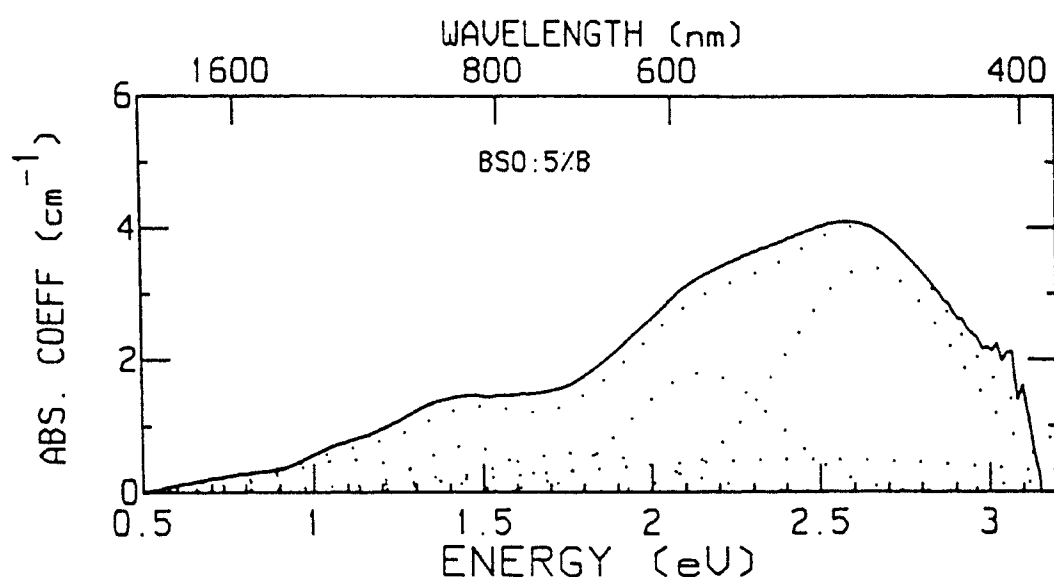Figure 7. The change in the absorption spectra for BSO:8% Boron.
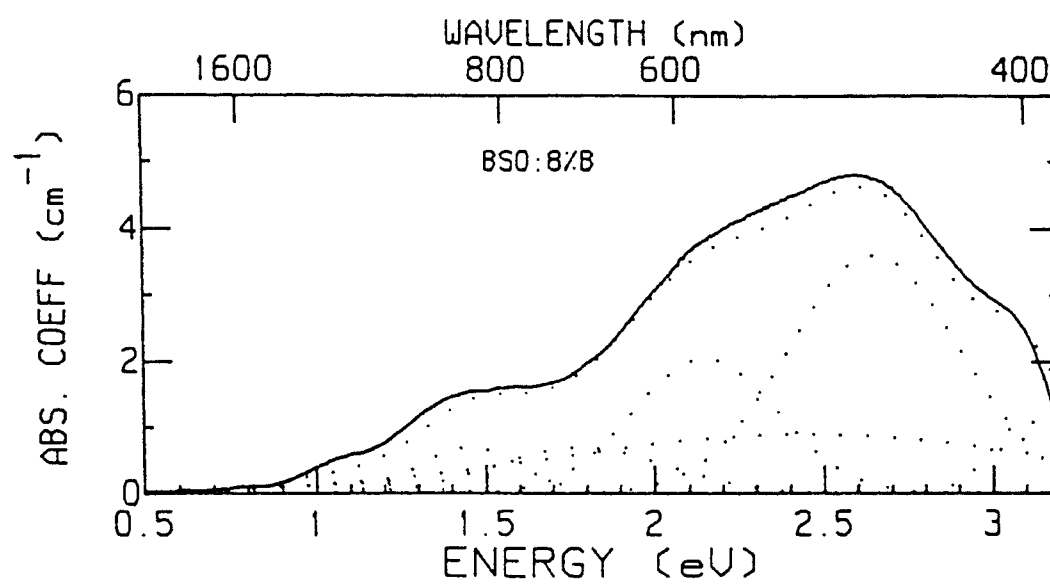
Figure 8. The Gaussian bands for BSO:5% Boron.

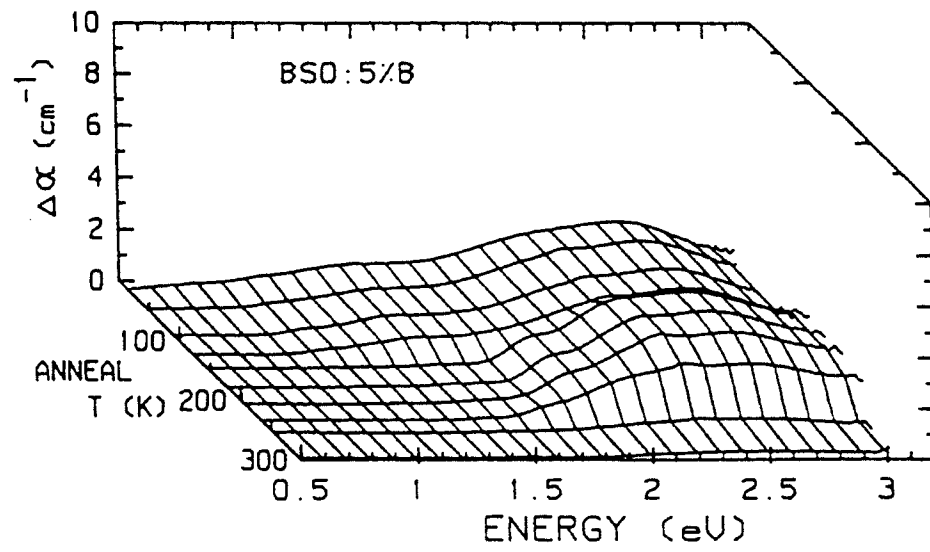Figure 9. The Gaussian bands for BSO:8% Boron.

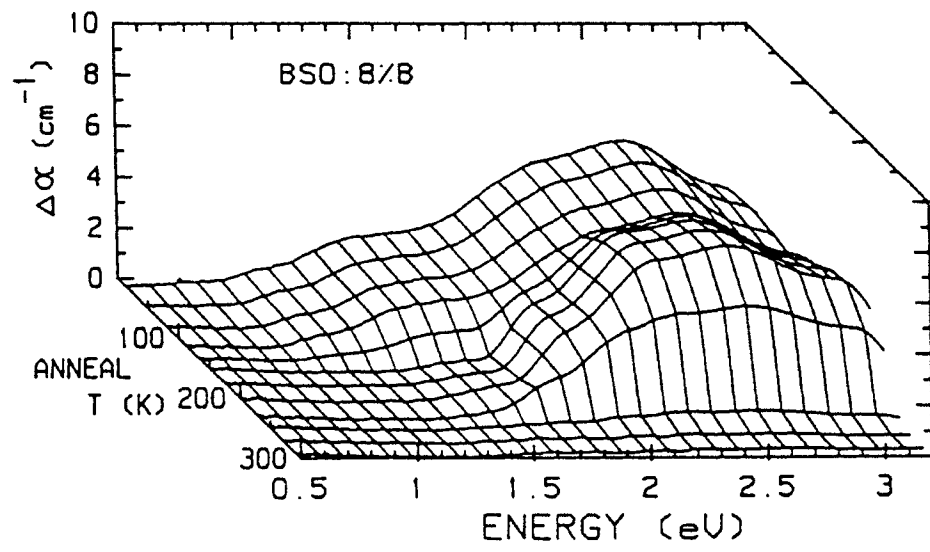Figure 10. The isochronal anneal contour plot for BSO:5% Boron.

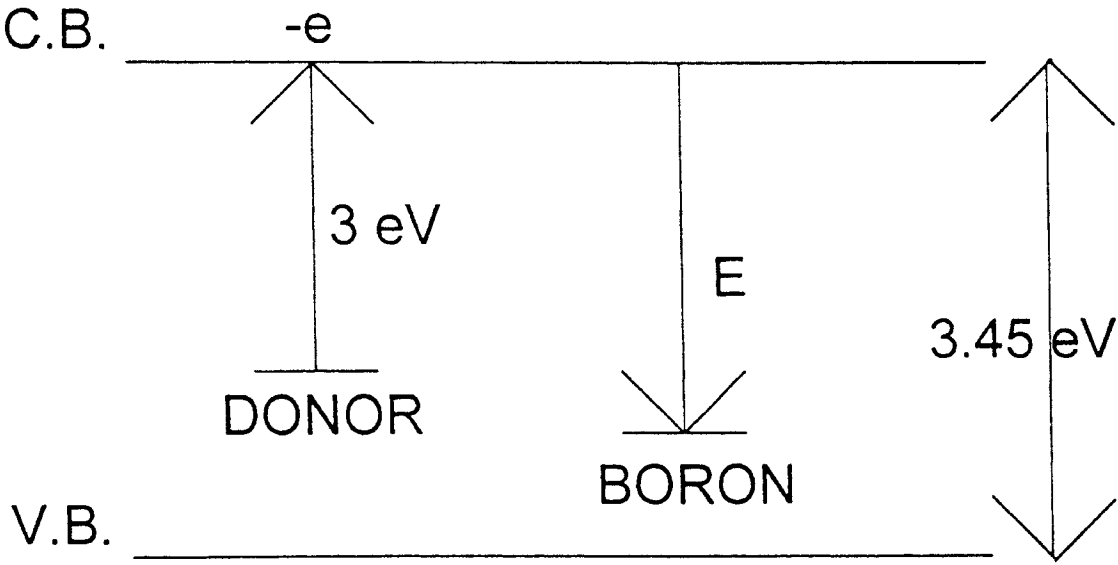Figure 11. The isochronal anneal contour plot for BSO:8% Boron.

Figure 12. Energy level diagram for BSO.

Photorefractive Effect

Several different experiments were performed on the photorefractive signal using the four-wave mixing set-up. The first experiment was designed to measure how the signal was affected by different shutter times at room temperature. The shutter was kept open for different amounts of time as the grating was being "written". Fig. 13 is for the 5% boron sample. This graph shows the dependence of the photorefractive signal on the time the shutter was open for each shutter run. It appears that the strength of the signal is independent of the "write" time when the shutter speed is between 0 and 1000 ms. Fig. 14 shows the same graph for the 8% boron sample. Again the strength of the signal seems to be independent of the shutter speed for shutter speeds between 0 and 1500 ms.

The next experiment used an attenuator between the HeCd laser and the beam splitter to vary the intensity of the "write" beam to see what effect this would have on the signal. Fig. 15 is a graph of the intensity of the photorefractive signal over time for the 5% boron sample when the "write" beam was at a power of 40 mW. The shutter speed was kept at a constant 100 ms. The leading edge peak became steadier as time increased. Fig. 16 is a graph of the intensity of the signal over time for different power settings of the "write" beam. This graph clearly shows a decrease in the photorefactive signal with a decrease in the power setting of the "write" beam. Figs. 17 and 18 are the same two graphs for the 8% boron sample. Here, the shutter speed was also kept at a constant 100 ms. Fig. 17 is a graph of the intensity of the signal over time for a power setting of 30 mW for the "write" beam. There is a small leading edge peak which quickly becomes steady. Fig. 18 is a log graph showing the intensity of the signal for different power

settings of the "write" beam. This graph is not nearly as clear as the one for the 5% sample. Still, there is a general decrease in the intensity of the signal with a decrease in the power of the "write" beam.
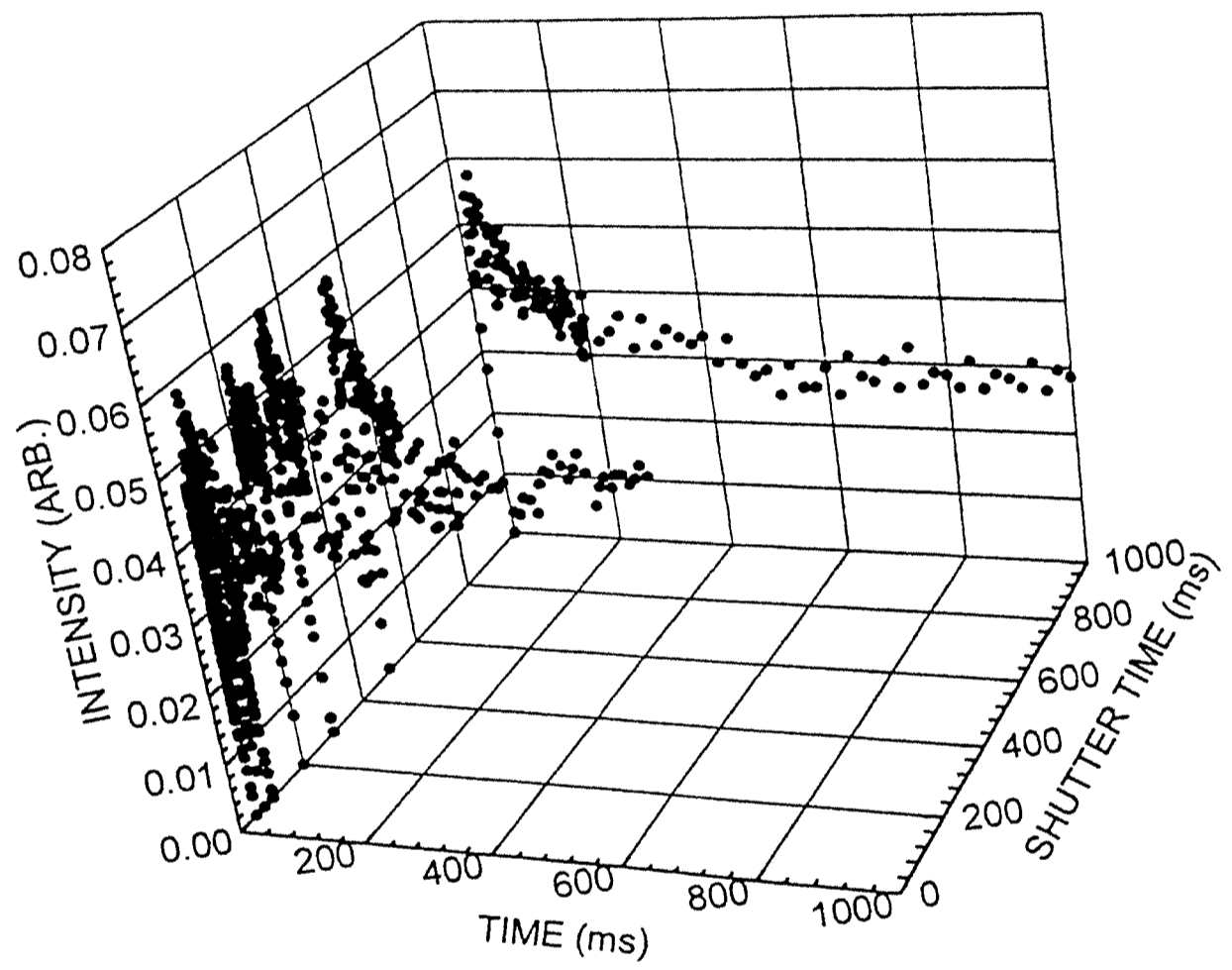
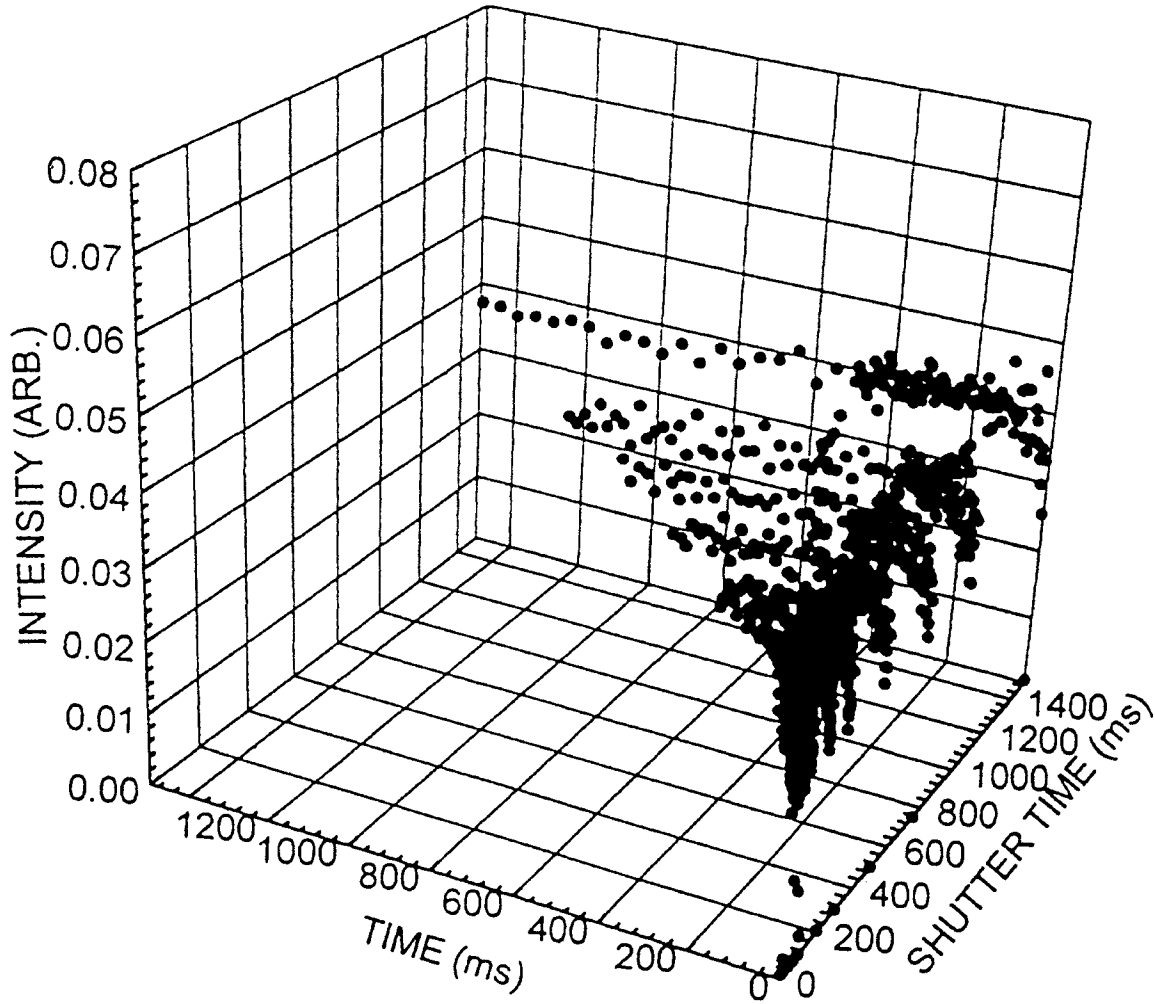Figure 13. Shutter runs for BSO:5% Boron.

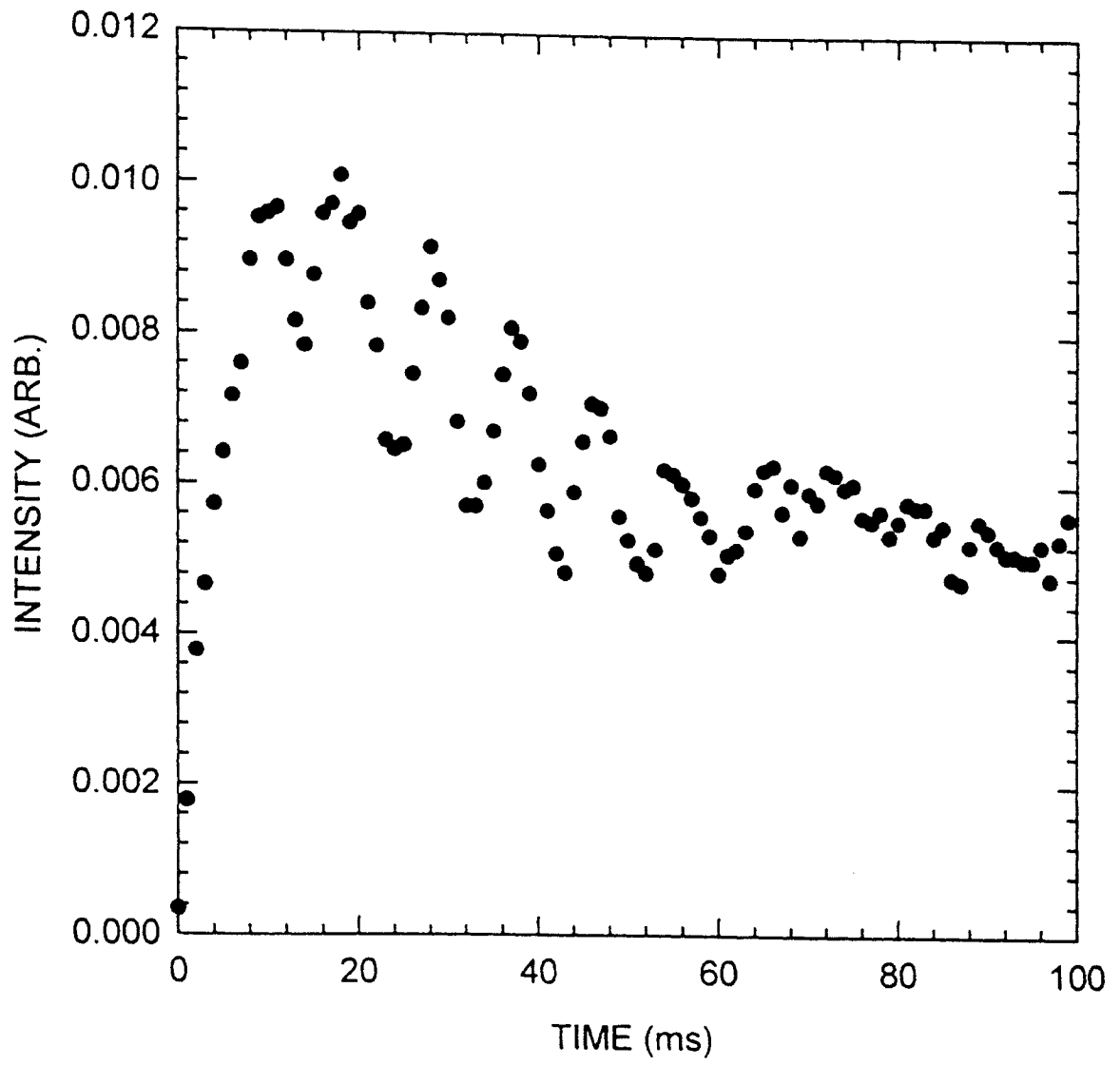Figure 14. Shutter runs for BSO:8% Boron.

Figure 15. The effect on the signal for BSO:5% Boron, using a 40 mW "write" beam.
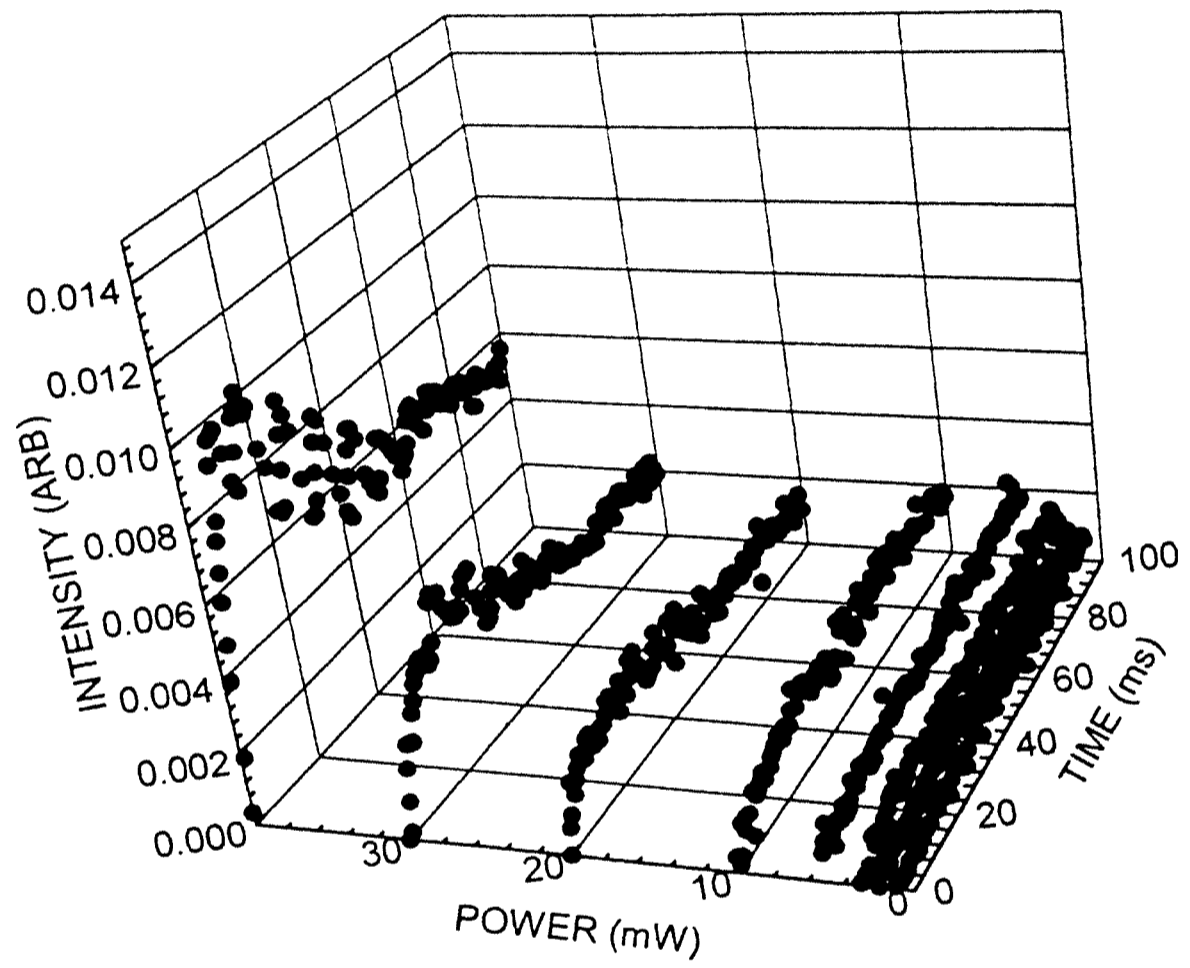
Figure 16. The effect on the signal for BSO:5% Boron, using different powers for the "write" beam.
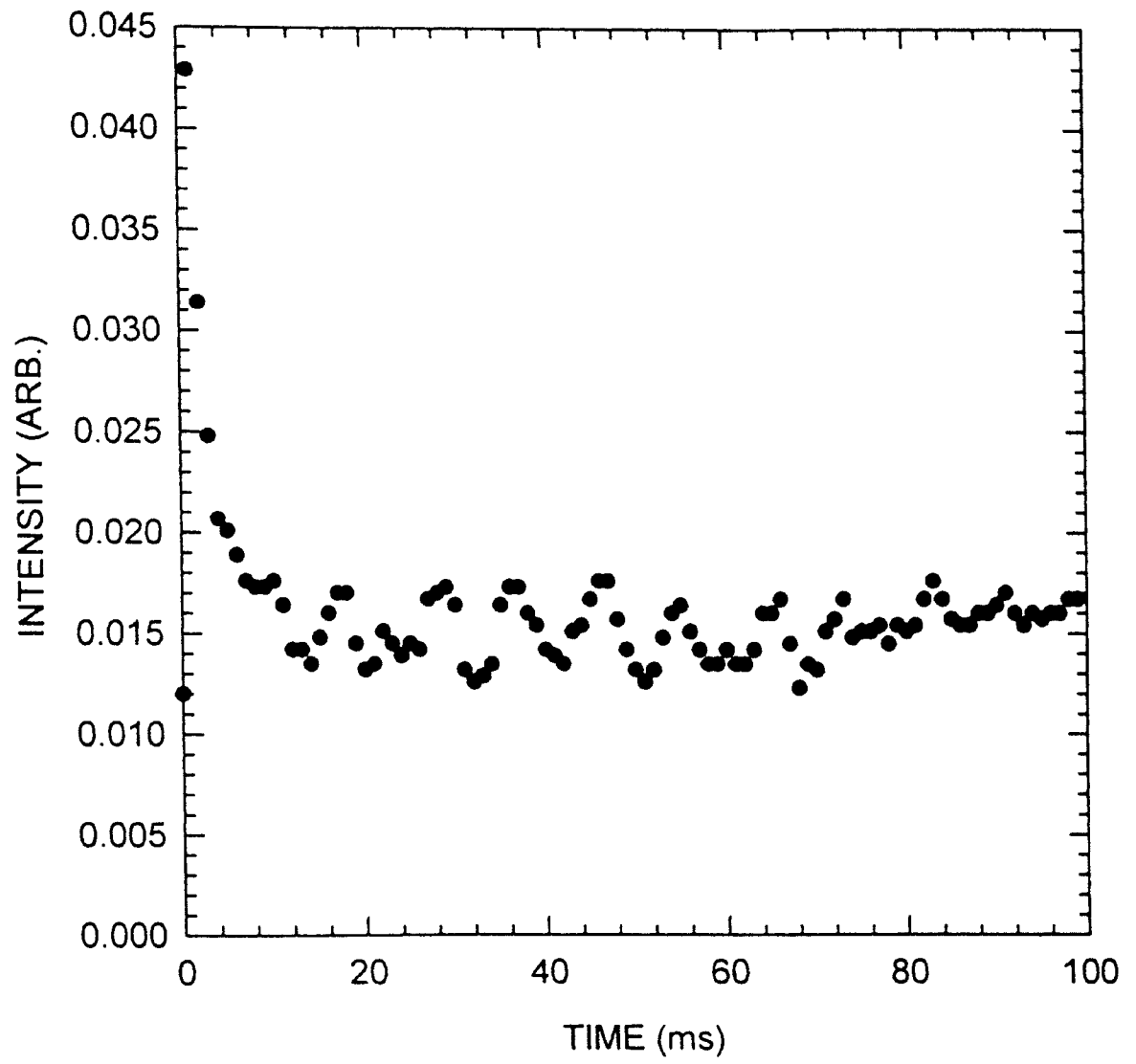
Figure 17. The effect on the signal for BSO:8% Boron, using a 30 mW "write" beam.
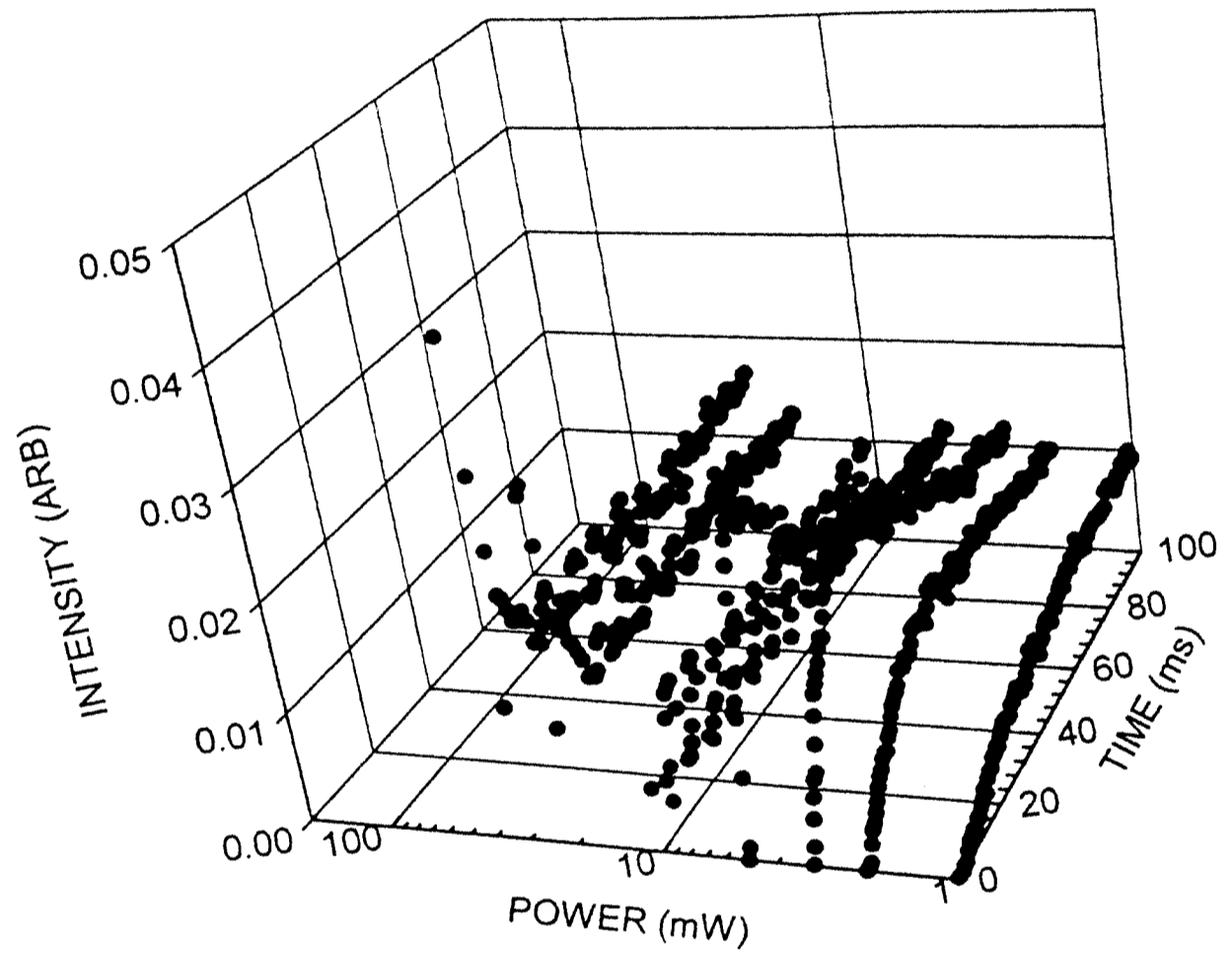
Figure 18. The effect on the signal for BSO:8% Boron using different powers for the "write" beam.

The third experiment measured the intensity of the signal as the temperature of the sample was decreased. Figs. 19 and 20 show this temperature and time dependence for the photorefractive signal for the 5% and 8% boron samples respectively. For the 5% sample, there occurred a steady increase in the signal as the temperature decreased until a peak was reached at a temperature of about 125 K. From that point, the signal began to decrease again as the temperature was further decreased, until it had dropped to nearly 0. The leading edge peak of the signal began to steady out as the temperature was decreased. The 8% sample produced similar, although not identical, results. The same increase in signal with the decrease in temperature was observed but this time the peak in signal was reached at a temperature of 75 K rather than 125 K. The signal did decrease after that temperature but it did not drop to 0 by 25 K as the 5% sample did. Again the leading edge peak became steadier as the temperature was decreased. The peaks in the signal may correspond to the decay of the infrared photochromic bands and the enhancement of the bands in the same approximate temperature region. The above results are different from those obtained for undoped BSO [25]. The photorefractive signal for undoped BSO experiences a steady growth in intensity. No decrease in the signal is observed.

At low temperatures, the grating "persisted" when the "write" beams were turned off. The final experiment measured the stability of the persistent grating. A grating was written at low temperature and then the temperature was steadily increased to approximately 200 K to see the effect on the photorefractive signal. Fig. 21 shows the direct dependence of the intensity of the persistent grating on temperature. Most of the grating's decay occurs before 100 K for both samples. The grating in the 5% boron

sample has stopped decaying by this temperature while the 8% boron sample is still experiencing a slow steady decay until about 175 K. Both samples show similar trends in intensity. For higher temperatures the gratings have lower intensities and for lower temperatures the gratings have higher intensities. Fig. 22 is a graph of the intensity of the two gratings plotted against 1000/temperature. This choice of variable will allow us to calculate the activation energy below. It can be seen from this graph that both signals experience a slow, steady decline until a point is reached. After this point, there is a more rapid decline. For the 5% sample, this point is at approximately 65 K and for the 8% sample the point is reached at approximately 55 K. A comparison with a similar plot for undoped BSO reveals that the same trend occurs [25]. The change in the slope in the undoped case is also at 55-65 K. Optical erasure probably accounts for some of the decay at low temperatures.

From Fig. 22 it is possible to calculate the activation energy of the trapped carriers. It is known that the relation between the intensity of the photorefractive signal and the temperature is given by

$$I = I_o \exp(E/kT),$$

where I is the intensity, I_o is the initial intensity, k is Boltzmann's constant (8.625×10^{-5} eV/K) and T is the temperature. Taking the natural log of both sides of the equation and inserting a factor of 1000, the following equation is obtained

$$\ln I = \ln I_o + (E/1000k)(1000/T).$$

This equation has the form of a straight line where ln I is the y-coordinate from the graphs, (1000/T) is the x-coordinate from the graphs, and (E/1000k) is the slope of the

line. A tangent line is drawn to the steep portion of the graphs and the slope is found. From the equation

$$slope=(E/1000k)$$

the activation energies can be calculated. For the 5% boron sample, the activation energy is 29 meV and for the 8% sample the activation energy is 37 meV. For undoped BSO, the activation energy was found to be 50 meV [25].

In all of the above results, the intensity is dependent on the prior "history" of the sample. This includes previous gratings written to the sample that may not have completely decayed. The intensity is also dependent on the time the "read" beam is exposed to the sample because of optical erasure.
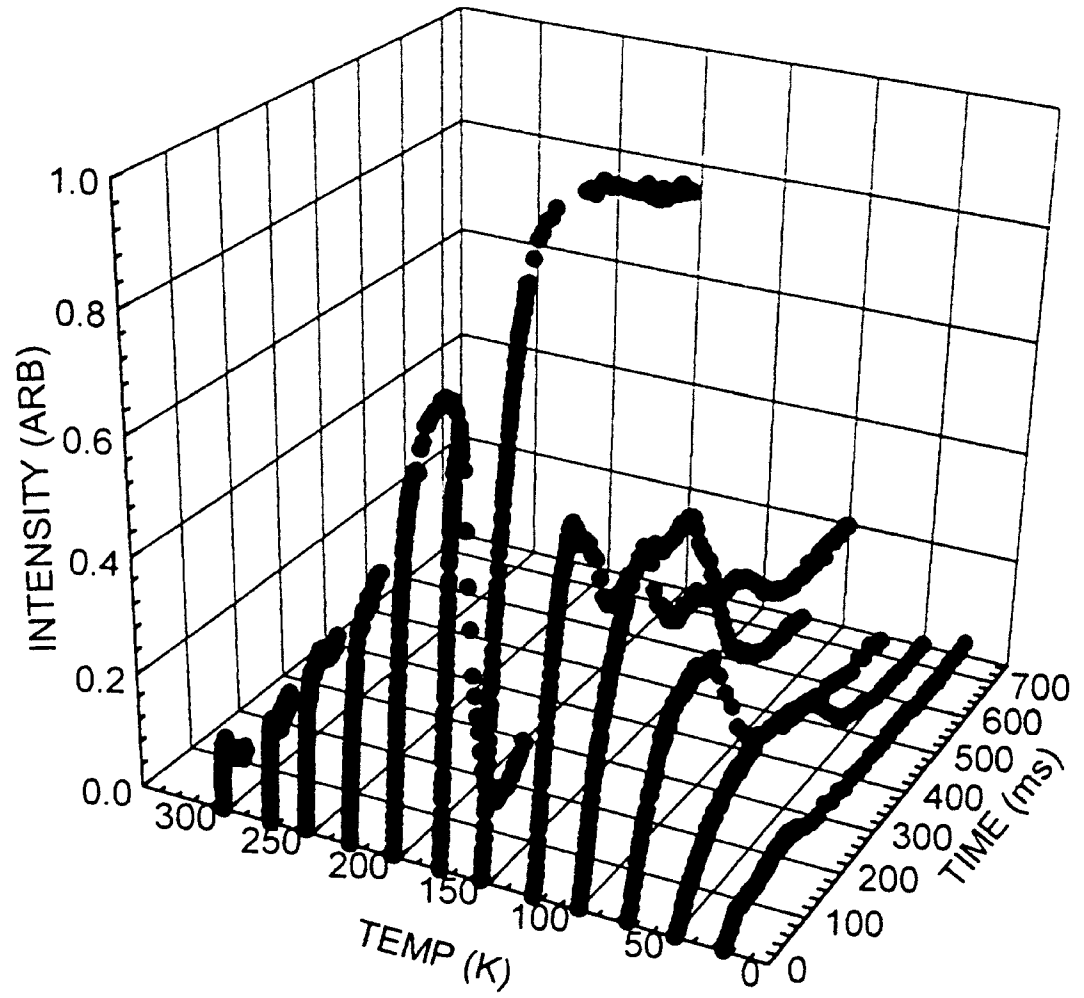
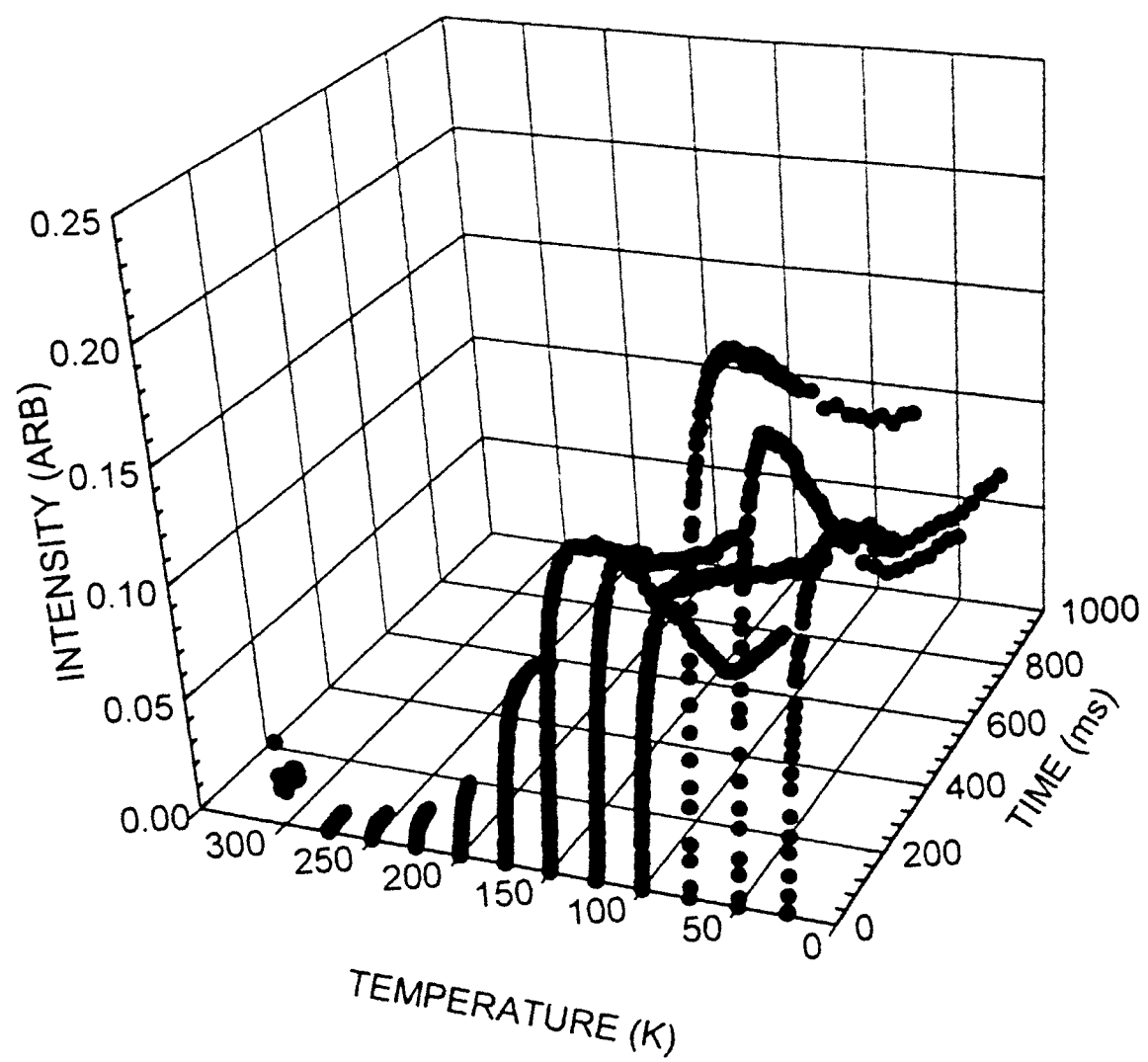Figure 19. The temperature dependence of BSO:5% Boron.

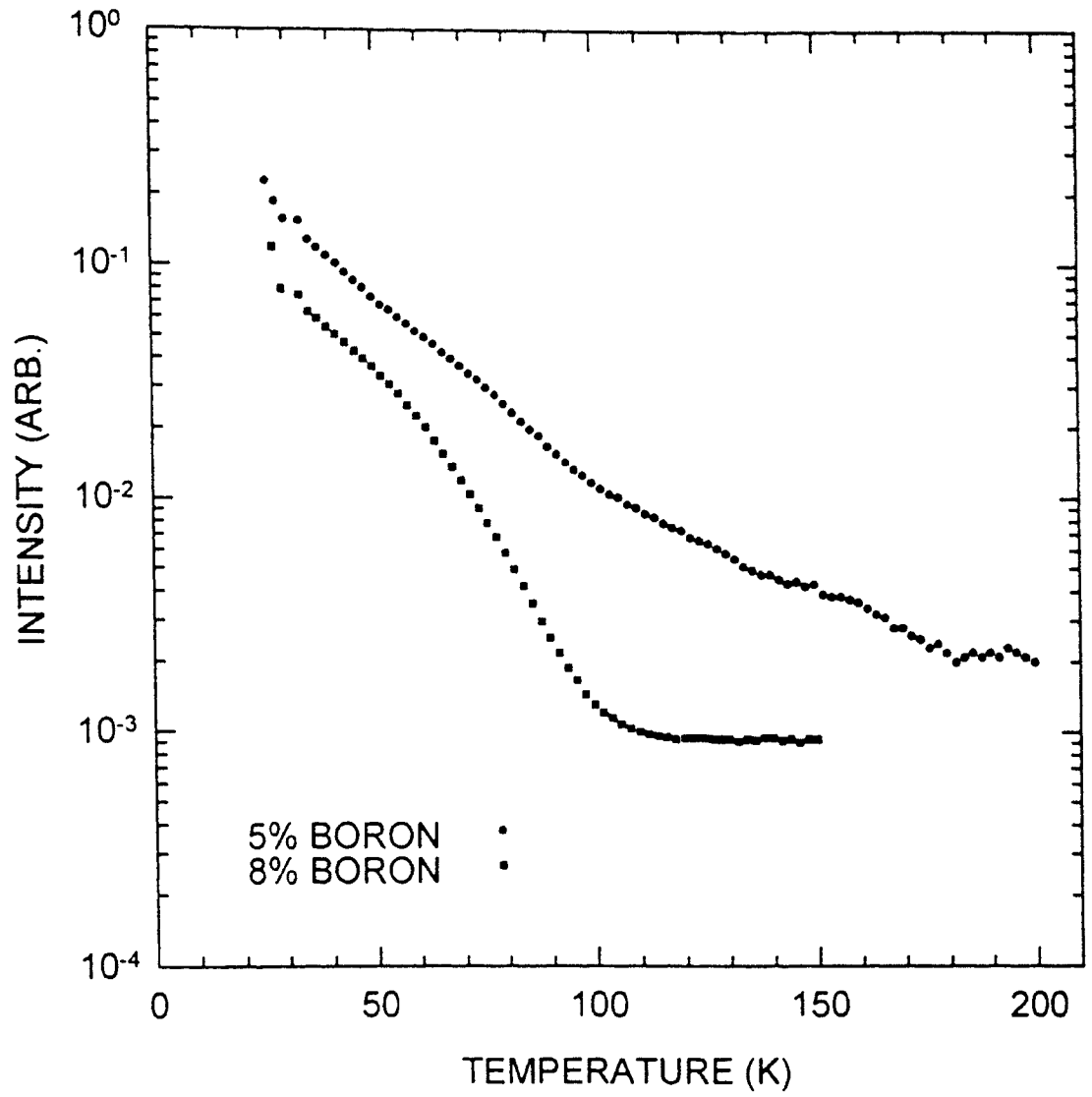Figure 20. The temperature dependence of BSO:8% Boron.

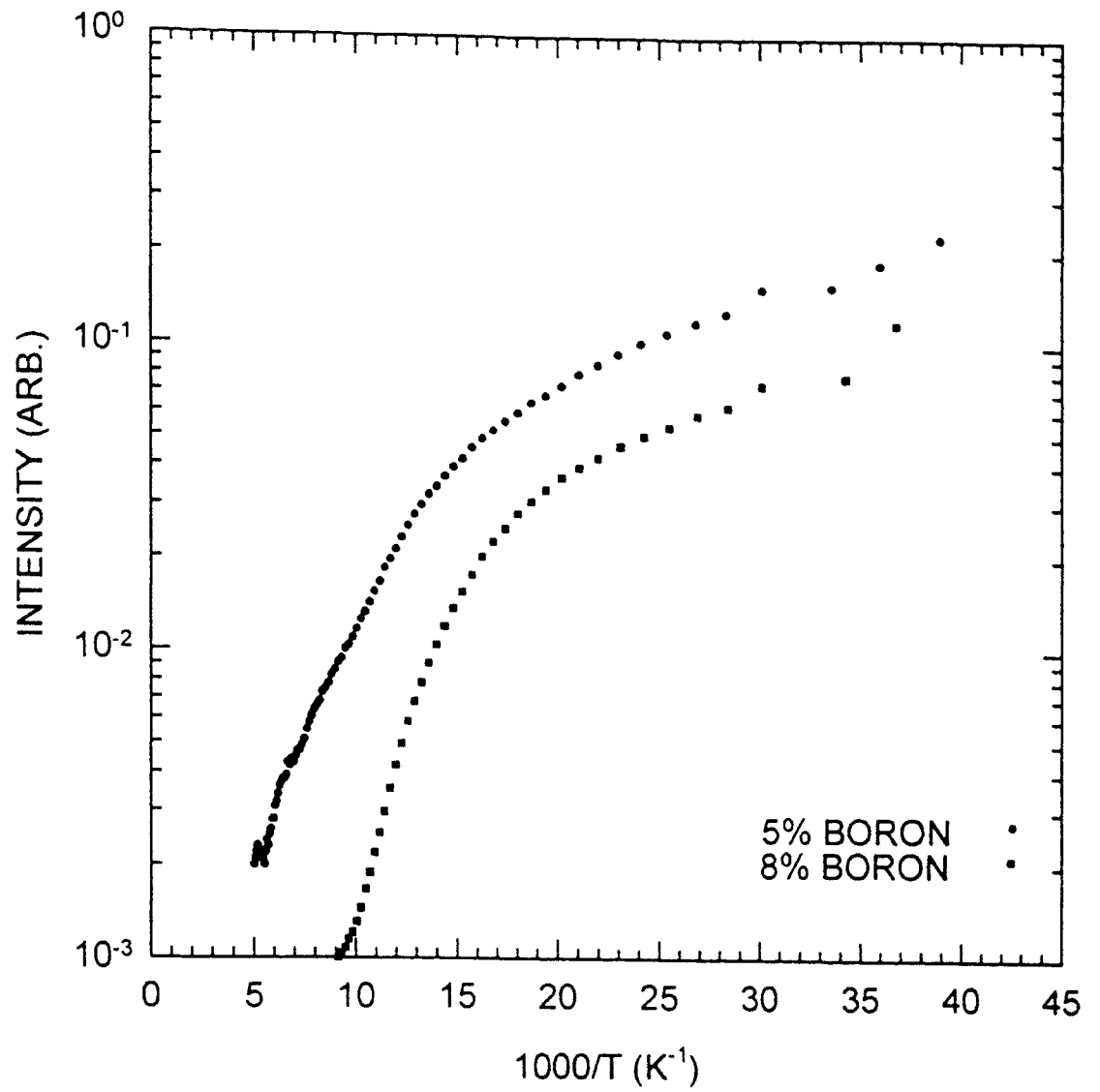Figure 21. The dependence of the intensity of the photorefractive grating on temperature.

Figure 22. Calculating the activation energy from the persistence of the photorefractive grating.

CHAPTER IV

CONCLUSION

Boron-doped BSO behaves essentially as undoped BSO. It may be impossible to fully compensate the deep donor with boron because the bonding radius for boron is significantly shorter than for silicon, aluminum, or gallium. Nevertheless, higher concentrations of boron should be added to the melt to test this hypothesis.

BSO doped with 5% and 8% boron form photochromic absorption bands when exposed to near-band-edge light at low temperatures. It was expected that doping with boron would fully compensate the absorption shoulder as doping with aluminum and gallium does. However, the photochromic bands for boron-doped bear a strong resemblance to those obtained for undoped BSO. These results are further strengthened by comparing the Gaussian bands obtained for the boron-doped samples with those obtained for undoped BSO.

The photorefractive measurements carried out on the two boron-doped samples also provide results similar to those for undoped BSO. The temperature dependence results for the boron-doped samples, however, show a decrease in intensity in the approximate temperature region where the infrared bands decay and the visible bands are enhanced. No similar decrease is seen in the undoped BSO sample.

REFERENCES

1.   R. E. Aldrich, S. L. Hou, and M. L. Harvill, J. Applied Physics **42**, 493 (1971).

2.   R. B. Lauer, Appl. Physics Letters **17**, 178 (1970).

3.   R. B. Lauer, J. Applied Physics **42**, 2147 (1971).

4.   A. Feldman, W. S. Brower, Jr., and B. Horowitz, Appl. Physics Letters **16**, 201 (1970).

5.   I. Arizmendi, J. M. Cabrera, and F. Aguillo-Lopez, Intl. J. Optoelectronics **7**, 149 (1992).

6.   M. T. Harris, J. J. Larkin, and J.J Martin, Appl. Physics Letters **60**, 2162 (1992).

7.   S. L. Hou, R. B. Lauer, and R. E. Aldrich, J. Applied Physics **44**, 2652 (1973).

8.   R. C. Grabmaier and R. Oberschmid, Phys. Stat. Sol. **96**, 199 (1986).

9.   W. Rehwald, K. Frick, G. K. Lang, and E. Meier, J. Applied Physics **47**, 1292 (1976).

10. R. Oberschmid, Phys. Stat. Sol. **89**, 263 (1985).

11. S. C. Abrahams, J. L. Bernstein, and C. Svensson, J. Chem. Physics **71**, 788 (1979).

12. H. J. Reyher, U. Hellwig, and O. Thiemann, Physical Review B **47**, 5638 (1993).

13. M. G. Jani and L. E. Halliburton, J. Applied Physics **64**, 2022 (1988).

14. D. W. Hart, C. A. Hunt, D. D. Hunt, J. J. Martin, M. T. Harris, and J. J. Larkin, J. Applied Physics **73**, 1443 (1993).

15. J. J. Martin, I. Foldvari, and C. A. Hunt, J. Applied Physics **70**, 7554 (1991).

16. D. W. Hart, C. A. Hunt, and J. J. Martin, J. Applied Physics **73**, 3974 (1993).

17. J. A. Weil, Phys. Chem. Minerals **10**, 149 (1984).

18. J. J. Martin, private communication, June 1994.

19. J. P. Huignard and F. Micheron, Applied Physics Letters **29**, 591 (1976).

20. P. Gunter, Physics Reports **93**, 199 (1982).

21. J. Feinberg, Optical Phase Conjugation, edited by Robert A. Fisher, (Academic Press, 1983).

22. I. Foldvari, J. J. Martin, C. A. Hunt, R. C. Powell, R. J. Reeves, and S. A. Holmstrom, Optical Materials **2**, 25 (1993).

23. C. Kittel, Introduction to Solid State Physics, 76, (John Wiley & Sons, Inc., 1986).

24. D. C. Craig and N. C. Stephenson, J. Solid State Chem. **15**, 1 (1975).

25. J. J. Martin, D. W. Hart, S. Hoefler, J. McCullough, and G. S. Dixon, Cleo '94 Technical Digest Series Conference Edition, 100.

VITA

Anne Marie Georgalas

Candidate for the Degree of

Master of Science

Thesis: A STUDY THE OF PHOTOCHROMIC AND PHOTOREFRACTIVE EFFECTS IN BORON-DOPED BISMUTH SILICON OXIDE

Major Field: Physics

Biographical:

Personal Data: Born in Columbus, Ohio, on May 17, 1969, the daughter of George and Mary Georgalas.

Education: Graduated from Berea High School, Berea, Ohio, June 1987; received Bachelor of Science degree in Physics from Cleveland State University, Cleveland, Ohio, June 1992; completed requirements for the Master of Science degree at Oklahoma State University, December 1994.

Professional Experience: Teaching Assistant, Department of Physics, Oklahoma State University, August 1992 to May 1994; Research Assistant, Department of Physics, Oklahoma State University, June 1993 to present.